

U.S. Department of Energy
FreedomCAR and Vehicle Technologies, EE-2G
1000 Independence Avenue, S.W.
Washington, D.C. 20585-0121

FY 2005

**BOOST CONVERTERS FOR GAS ELECTRIC AND
FUEL CELL HYBRID ELECTRIC VEHICLES**

Prepared by:

Oak Ridge National Laboratory

Mitchell Olszewski, Program Manager

Submitted to:

**Energy Efficiency and Renewable Energy
FreedomCAR and Vehicle Technologies
Vehicle Systems Team**

Susan A. Rogers, Technology Development Manager

June 2005

Engineering Science & Technology Division

**BOOST CONVERTERS FOR
GAS ELECTRIC AND FUEL CELL
HYBRID ELECTRIC VEHICLES**

**J. W. McKeever
S. C. Nelson
G. J. Su**

Publication Date: June 2005

Prepared by the
OAK RIDGE NATIONAL LABORATORY
Oak Ridge, Tennessee 37831
managed by
UT-BATTELLE, LLC
for the
U.S. DEPARTMENT OF ENERGY
Under contract DE-AC05-00OR22725



This report was prepared as an account of work sponsored by an agency of the United States Government. Neither the United States Government nor any agency thereof, nor any of their employees, makes any warranty, express or implied, or assumes any legal liability or responsibility for the accuracy, completeness, or usefulness of any information, apparatus, product, or process disclosed, or represents that its use would not infringe privately owned rights. Reference herein to any specific commercial product, process, or service by trade name, trademark, manufacturer, or otherwise, does not necessarily constitute or imply its endorsement, recommendation, or favoring by the United States Government or any agency thereof. The views and opinions of authors expressed herein do not necessarily state or reflect those of the United States Government or any agency thereof.

TABLE CONTENTS

	Page
LIST OF FIGURES	iii
LIST OF TABLES	iii
ACROYNMS	iv
INTRODUCTION	1
BACKGROUND	1
OPERATION OF THE BOOST, BUCK, AND BI-DIRECTIONAL FEATURES OF THE CHOPPER	2
PWM AND THE VOLTAGE SOURCE INVERTER	4
THE Z-SOURCE INVERTER	6
DISCUSSION	12
CONCLUSIONS	21
REFERENCES	23
DISTRIBUTION	24

LIST OF FIGURES

Figure		Page
1	Two quadrant bi-directional chopper similar to the one used in THSII	3
2	Boost operation	3
3	Buck operation to charge battery	4
4	One phase of control voltage waveforms to modulate pulse widths	5
5	Three-phase inverter	6
6	Z-source inverter	6
7	Equivalent circuits of the Z-source inverter	8
8	Relation between shoot-through and PWM indexes	9
9	Three-phase PWM and boost control curves showing maximum constant boost envelopes	10
10	Relation of boost and gain to PWM index	11
11	Schematic similar to THS	12
12	Schematic similar to THSII	13
13	Conventional boost converter configuration of a FC powered HEV	14
14	Simple and complex FC powered EVs	14
15	Proposed configuration of a Z-source inverter driven FC HEV	15
16	A configuration of an ICE powered HEV driven by a Z-source inverter	16

LIST OF TABLES

Table		Page
1	Component count for several HEV configurations with and without voltage boost	17
2	Estimated cost of power build section of several EV and HEV inverter configurations	20

ACRONYMS

ac	alternating current
dc	direct current
CMEU	compressor motor expanding unit
DMIC	dual mode inverter control
EMI	electromagnetic interference
EV	electric vehicle
FC	fuel cell
HEV	hybrid electric vehicle
ICE	internal combustion engine
IGBT	insulated gate bipolar transistor
MSU	Michigan State University
OEM	original equipment manufacturer
ORNL	Oak Ridge National Laboratory
PWM	pulse width modulation
SDP	switching device power
SOC	state-of-charge
THS	Toyota Hybrid System (first)
THSII	Toyota Hybrid System (new generation)
V-source	voltage-source
I-source	current-source

INTRODUCTION

Hybrid electric vehicles (HEVs) are driven by at least two prime energy sources, such as an internal combustion engine (ICE) and propulsion battery. For a series HEV configuration, the ICE drives only a generator, which maintains the state-of-charge (SOC) of propulsion and accessory batteries and drives the electric traction motor. For a parallel HEV configuration, the ICE is mechanically connected to directly drive the wheels as well as the generator, which likewise maintains the SOC of propulsion and accessory batteries and drives the electric traction motor. Today the prime energy source is an ICE; tomorrow it will very likely be a fuel cell (FC). Use of the FC eliminates a direct drive capability accentuating the importance of the battery charge and discharge systems. In both systems, the electric traction motor may use the voltage directly from the batteries or from a boost converter that raises the voltage. If low battery voltage is used directly, some special control circuitry, such as dual mode inverter control (DMIC) which adds a small cost, is necessary to drive the electric motor above base speed. If high voltage is chosen for more efficient motor operation or for high speed operation, the propulsion battery voltage must be raised, which would require some type of two-quadrant bi-directional chopper with an additional cost.

Two common direct current (dc)-to-dc converters are: (1) the transformer-based boost or buck converter, which inverts a dc voltage, feeds the resulting alternating current (ac) into a transformer to raise or lower the voltage, and rectifies it to complete the conversion; and (2) the inductor-based switch mode boost or buck converter [1]. The switch-mode boost and buck features are discussed in this report as they operate in a bi-directional chopper. A benefit of the transformer-based boost converter is that it isolates the high voltage from the low voltage. Usually the transformer is large, further increasing the cost. A useful feature of the switch mode boost converter is its simplicity. Its inductor must handle the entire current, which is responsible for its main cost. The new Z-source inverter technology [2,3] boosts voltage directly by actively using the zero state time to boost the voltage. In the traditional pulse width modulated (PWM) inverter, this time is used only to control the average voltage by disconnecting the supply voltage from the motor. The purpose of this study is to examine the Z-source's potential for reducing the cost and improving the reliability of HEVs.

BACKGROUND

As part of an FY 2000 life cycle cost study [4], Oak Ridge National Laboratory (ORNL) estimated the cost of a boost converter to be the cost of an inverter reduced by the cost of the control components reasoning that the boost converter could be controlled by the same control components as the inverter. That cost added a significant cost penalty of \$240 to the control system. Applying the same approach to recent inverter technology, the cost penalty was dramatically reduced to \$149 in 2002 with a target of \$113. Apparently this penalty has not discouraged the engineers at the Toyota Motor Corporation, because in September 2003 the Toyota Motor Corporation introduced a second generation of the Toyota Hybrid System (THSII) which boasted a 50% improvement in motor power output [5], whose enabling feature was a two-quadrant bi-directional chopper placed between the inverter's system voltage and the batteries' output voltage.

Recently a new power converter topology was introduced that modifies a standard voltage fed or current fed PWM inverter and may be controlled to buck or boost not only dc-to-dc, but also dc-to-ac, ac-to-dc, and ac-to-ac. It is called a Z-source inverter [2,3] and it adds a network of impedance to eliminate the problem of shoot-through. Shoot-through, which shoots the supply voltage through an inverter's upper and lower semiconductor switches, destroys the switches and it must be prevented by time delays in the control circuit. The Z-source inverter actually uses shoot-through to boost the voltage. It makes more complete use of the available operating time of a PWM inverter, which will be explained in the section on the Z-source inverter.

The research objective of the Z-source inverter was to provide a monolithic inverter to connect a FC with the traction drive of an HEV. The boost feature is essential for FC operation because the static characteristics of FCs exhibit more than a 30% reduction in the output voltage between no-load and full-load current draw [6]. The buck feature in the opposite direction is needed because the storage batteries' SOC must be maintained.

OPERATION OF THE BOOST, BUCK, AND BI-DIRECTIONAL FEATURES OF THE CHOPPER

The boost and buck converters both use an inductor and control the duty cycles for current through that inductor to provide the desired relation between input and output voltages. Duty cycle is defined as the ratio of the time a switch is closed, T_o , to its total operating time per cycle, $T = (T_o + T_l)$, which is expressed as

$$D = T_o / (T_o + T_l) = T_o / T. \quad (1)$$

The voltage across an inductor is given by Lenz's law, $v = L di/dt$. Integration of this equation over one steady state period leads to the equation,

$$L \int_{i(t)}^{i(t+T)} di = \int_0^T v dt = 0, \quad (2)$$

because at the beginning and end of periodic steady state operation, the values of $i(t)$ are the same. The expression for the average value of v is

$$\bar{v} = \frac{1}{T} \int_0^T v dt = 0, \quad (3)$$

which is zero because of (2). The fact that the average voltage across an inductor is zero for periodic steady state operation is used to calculate the duty cycles for boost and buck operation.

The method of calculating the duty cycles for boost and buck will now be shown for a two quadrant bi-directional chopper like the one used in Toyota's THSII and illustrated in the Fig. 1 schematic.

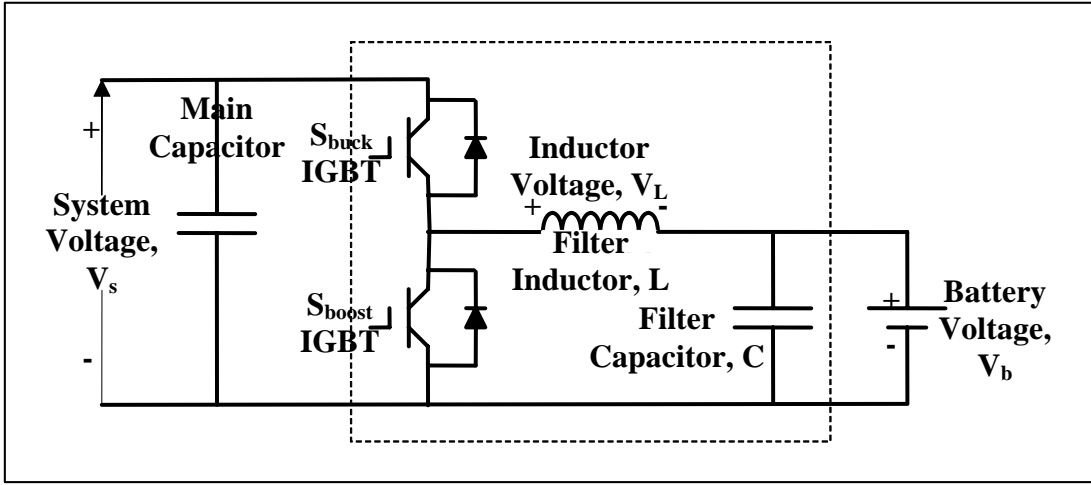


Fig. 1. Two-quadrant bi-directional chopper similar to the one used in THSII.

When the boost circuit operates, as shown in Fig. 2, the upper insulated gate bipolar transistor (IGBT) is omitted from the schematic because S_{buck} stays open. The upper IGBT's bypass diode, however, controls current to flow to the supply bus and remains part of the active boost circuit. In Fig. 2(a), S_{boost} is closed so that the voltage across the inductor equals the negative of the battery voltage and $di/dt < 0$. In Fig. 2(b), S_{boost} is opened so that the voltage across the inductor equals the system voltage minus the battery voltage and the $di/dt > 0$. V_s must be greater than V_b .

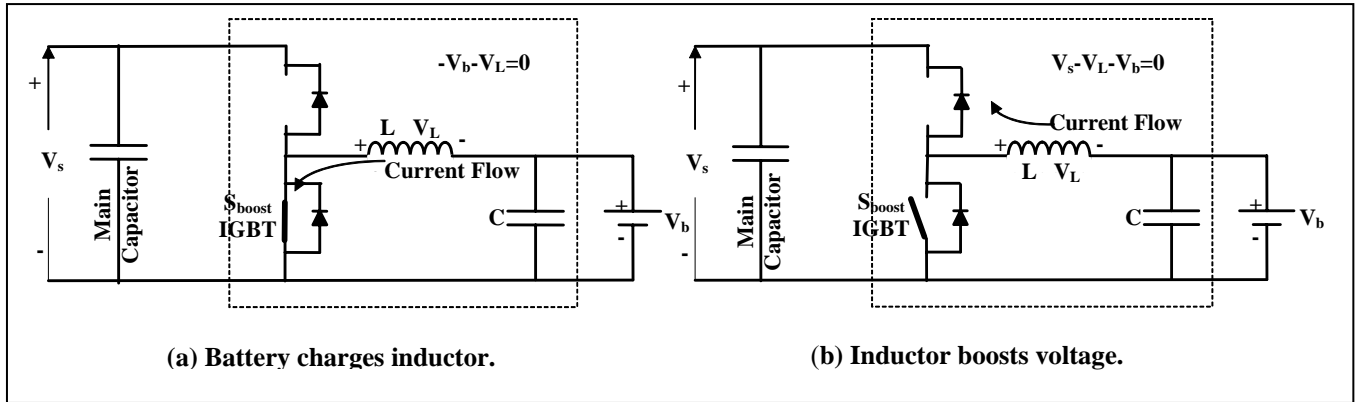


Fig. 2. Boost operation.

The expression for average voltage is

$$T_o(-V_b) + (T - T_o) \times (V_s - V_b) = 0, \quad (4)$$

which leads to the gain for boost operation with switch, S_{buck} , open,

$$\beta_{boost} = \frac{V_s}{V_b} = \frac{1}{(1 - D)}. \quad (5)$$

When the buck circuit operates, as shown in Fig. 3, the lower IGBT is omitted from the schematic because S_{boost} stays open. The lower IGBT's bypass diode, however, controls current flow to the supply bus and remains part of the active boost circuit. In Fig. 3(a), S_{buck} is closed so that the voltage across the inductor equals the system voltage minus the battery voltage and $di/dt > 0$. In Fig. 3(b), S_{buck} is opened so that the voltage across the inductor equals the negative of the battery and $di/dt < 0$.

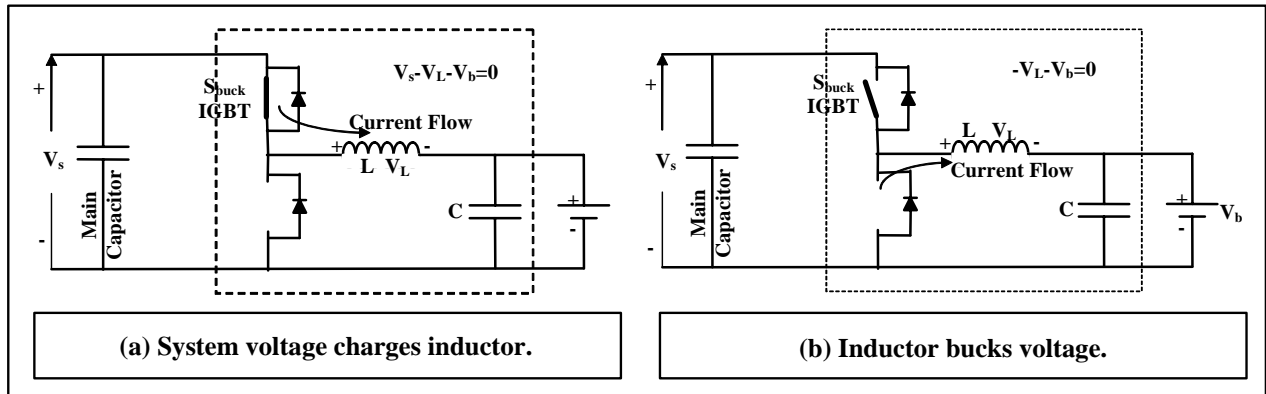


Fig. 3. Buck operation to charge battery.

The expression for average voltage (4) is $T_o(V_s - V_b) + (T - T_o) \times (-V_b) = 0$, which leads to the gain for buck operation with switch S_{boost} open,

$$\beta_{\text{buck}} = \frac{V_b}{V_s} = D \quad (6)$$

PWM AND THE VOLTAGE SOURCE INVERTER

PWM inverters control the turn-on and turn-off times of a dc supply voltage to synthesize both amplitude and frequency of sinusoidal voltage and resulting current waveforms when driving electric systems. When to turn the switches on and off is determined by comparing the voltage of a high frequency carrier wave, usually triangular or saw-tooth, with the voltage of a modulating wave, whose form it is desired to reproduce. Before power semiconductors made this possible, the voltage amplitude was controlled with transformers and the frequency was separately controlled by changing the frequency of the generator that fed the transformer.

A periodic control voltage waveform, called the modulating voltage, is selected for synthesis and superimposed on a much higher frequency carrier wave which is usually triangular, as shown in Fig. 4. Power electronic switches connected in an H-bridge, like the one shown in Fig. 5, connect a dc supply voltage to a load. When the switches are closed at t_{on} , the voltage time averaging over one carrier wave begins. Control of t_{on} and t_{off} is achieved by comparing the modulating voltage with the carrier voltage. When the magnitude of the carrier voltage exceeds the magnitude of the modulating voltage, one of the active switches is opened to end any further

contribution to the time average voltage. Similar triangles on the control plot of voltage vs. time show that $T/T_s = (V_{carrier} - V_{modulation})/V_{carrier}$. The average voltage at any time is

$$v_{average} = \frac{(T_s - T)}{T_s} \times \frac{V_{dc}}{2} = \frac{V_{modulation}}{V_{carrier}} \times \frac{V_{dc}}{2} = M \frac{V_{dc}}{2}, \quad (7)$$

where the modulation index, M , varies with time to synthesize the average voltage. If average voltage were plotted, it would look like the modulating voltage waveform.

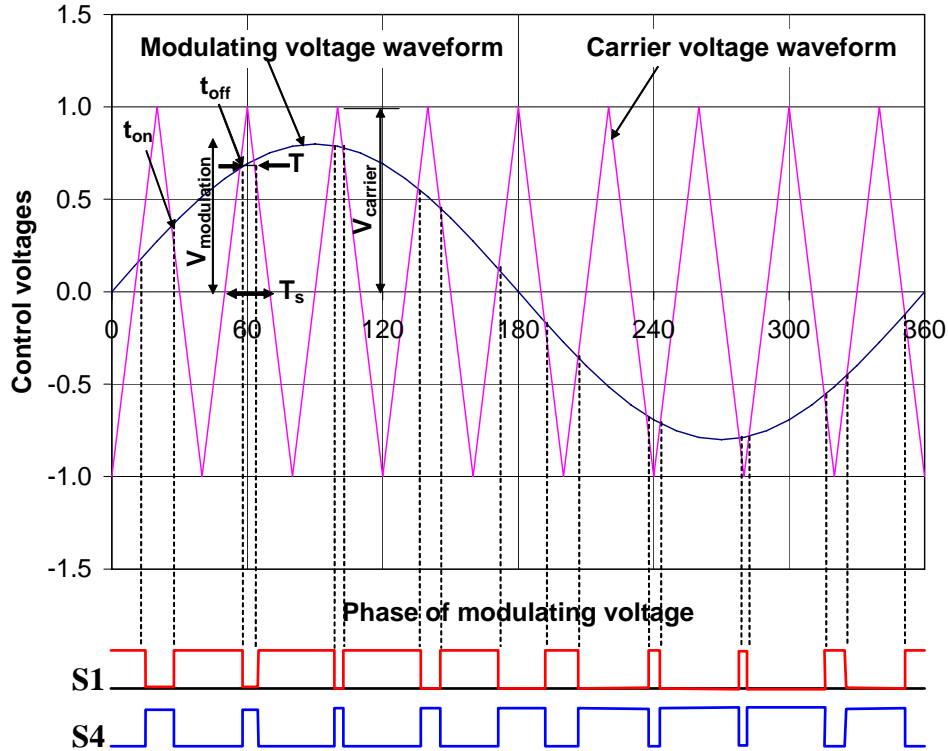


Fig. 4. One phase of control voltage waveforms to modulate pulse widths.

For the upper half of the modulating waveform, switches S1 and S6 are active and S1 is rapidly toggled by the carrier wave to achieve the desired average positive voltage. For the lower half of the modulating waveform, switches S3 and S4 become active and S3 is rapidly toggled to achieve the desired average negative voltage. This same method is used to synthesize each of the three voltage waveforms, which are separated by 120° in this three-phase system.

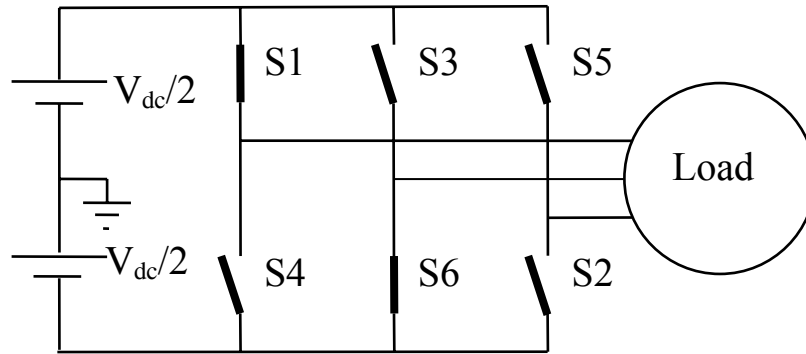


Fig. 5. Three-phase inverter.

THE Z-SOURCE INVERTER

Technology for the two traditional inverters, which are voltage-source (V-source) inverters and current-source (I-source) inverters, had been advanced by the invention of the Z-source inverter, which employs an impedance circuit to couple a power source to the input of an inverter [2,3]. The Z-source inverter provides a power conversion process that may be used to synthesize waveforms with voltages above as well as below the source voltage. Its use eliminates the switch or switches required by a boost converter. It can be applied to all dc-to-ac, ac-to-dc, ac-to-ac, and dc-to-dc power conversions.

Traditional V-source and I-source inverters have certain limitations not exhibited by the Z-source inverter. First, they may either boost or buck the voltage, but not both. Second, electromagnetic interference (EMI) induced misgating may cause shoot-through in a V-source inverter or may cause an open inductor circuit in the I-source inverter, which will destroy the switches. Dead time for the V-source inverter and overlap time for the I-source inverter causes waveform distortion.

Figure 6 shows a schematic of the Z-source converter. If a FC is used, the blocking diode has the additional task of preventing current flow back into the FC in addition to its boosting function.

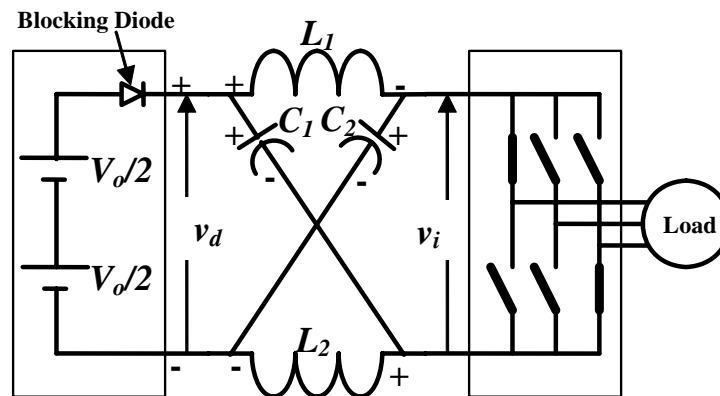


Fig. 6. Z-source inverter.

As already mentioned, the Z-source inverter makes more complete use of the available operating time of a PWM inverter. During traditional PWM, an active semiconductor switch is turned off to disconnect the V-source from the motor each time the magnitude of the triangular carrier voltage exceeds the magnitude of the modulating wave. It is not turned back on until the carrier wave falls back below the modulating wave. That time period is used by the traditional PWM inverter to synthesize the average voltage and may only allow the three upper switches or the three lower switches to be closed simultaneously to synthesize the average voltage. If an upper and lower switch in the same phase are closed, shoot-through occurs which could destroy the switches in that phase. These two permitted states, one with three upper switches on or one with three lower switches on, are called zero states and all they do is create a path for the motor current when the supply is disconnected. Because of the two inductances and two capacitors in the Z-source circuit, shoot-through is permitted allowing double use of what was formerly the zero vector time. Not only is this time used to control the average voltage, but it is also used to boost the voltage.

A FC produces voltage that can diminish considerably as more current is drawn from it [6]. To compensate for this, a dc-dc boost converter is traditionally required. The Z-source inverter functions as a single stage buck-boost inverter that can directly synthesize stable output voltage waveforms over a wide range of FC input voltages. This will now be explained.

Figure 7 shows two equivalent circuits of the Z-source inverter, one for the conventional non-shoot through states and a second for the shoot-through states. The voltage equalities in the figure are based on the sum of the voltages around a loop being zero and the voltages are positive when traversed from minus to plus. During non-shoot through, the voltage across the inductor is $v_L = V_o - v_c$. During shoot-through, the voltage across the inductor is $v_L = v_c$. If T_o and T_I are the shoot-through and non-shoot-through times respectively, the zero average inductor voltage over one carrier cycle from (3) is

$$\bar{v}_L = 0 = \frac{T_o \times v_c + T_I \times (V_o - v_c)}{T_o + T_I}, \quad (8)$$

which leads to the relationship between the supply voltage and the capacitor voltage,

$$\frac{v_c}{V_o} = \frac{T_I}{T_I - T_o}. \quad (9)$$

The average link voltage across the inverter bridge is

$$\bar{v}_i = \frac{T_o \times 0 + T_I \times (2v_c - V_o)}{T_o + T_I} = \frac{T_I}{T_I - T_o} V_o = v_c. \quad (10)$$

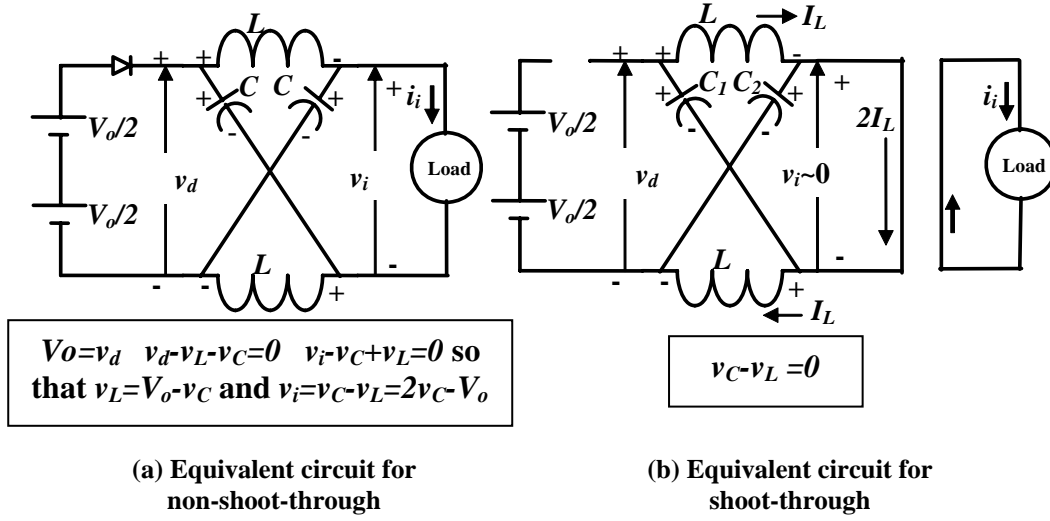


Fig. 7. Equivalent circuits of the Z-source inverter.

With the help of (9), the link voltage may also be expressed as

$$v_i = (2v_C - V_o) = \frac{T_1 + T_o}{T_1 - T_o} V_o = \frac{T_{carrier}}{T_1 - T_o} V_o = B \times V_o, \quad (11)$$

where $T_{carrier} = T_o + T_1$ is the half-period of the carrier wave and B is the boost factor

$$B = \frac{T_{carrier}}{T_1 - T_o} = \frac{1}{1 - 2 \frac{T_o}{T_{carrier}}} \geq 1. \quad (12)$$

Since the phase voltage output of the inverter is related to the link voltage by (7), (12) may be used to relate the source input voltage, V_o , to the output phase voltage as

$$v_{phase} = B \times M \times \frac{V_o}{2}, \quad (13)$$

where M is the PWM index and the system gain is $G = BM$. The traditional V-source PWM inverter equation is (12) with $B = 1$. Equation (13) shows how the Z-source inverter can function as a boost converter when connecting a FC, whose voltage drops as current increases, to a high-voltage motor without requiring a separate boost converter.

Figure 8 shows how the similar triangles formed on a superposition of the high frequency carrier voltage over the low frequency PWM voltage relate the shoot-through duty ratio, $T_o/T_{carrier}$, to the reference voltage used to determine shoot-through. The similar triangles lead to the relation,

$$\frac{T_o}{T_{carrier}} = \frac{V_{carrier} - V_{ref}}{V_{carrier}} = 1 - M_{shoot-through} \quad (14)$$

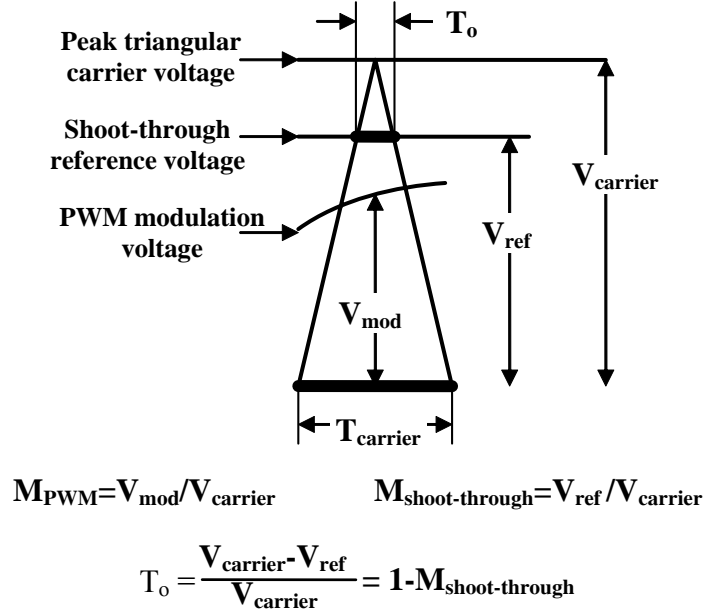


Fig. 8. Relation between shoot-through and PWM indexes.

As the reference voltage approaches, the envelope of the modulation waveforms, T_o , increases. Its maximum value occurs when V_{ref} and V_{mod} are equal, which occurs when $M_{shoot-through} = M$. When these modulation indices are equal, shoot-through is allowed to occupy the full PWM cutoff time. It cannot be larger because shoot-through would begin affecting the time average voltage whose control is the goal of PWM. Consequently, the maximum value of B is $1/(2M-1)$ leading to the inequality,

$$B \leq \frac{1}{2M - 1} \quad (15)$$

which shows that the maximum boost may be increased by reducing M .

In the foundational paper [4], the value of T_o was a constant which was determined by the intersection of a horizontal reference voltage with the carrier voltage. The value of V_{ref} fell outside of the envelope of the PWM voltage. Two subsequent analyses addressed boost control of the Z-source inverter. The first derived a maximum boost control [8], which is really a maximum average boost control. The second derived a maximum constant boost control [9], which is important because it does not infringe on PWM control. The following discussion of boost control values of V_{ref} is based on Fig. 9, which superposes a common carrier wave over the three-voltage waveforms used to PWM a three-phase system.

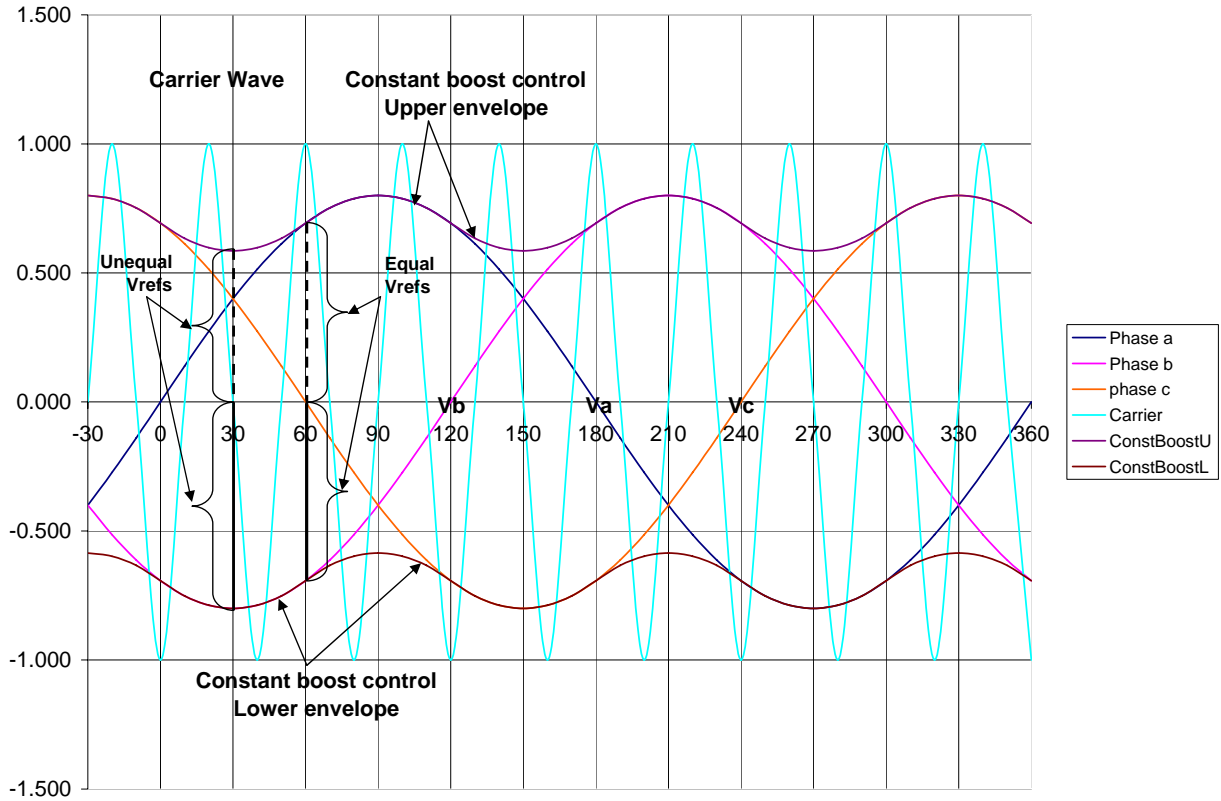


Fig. 9. Three-phase PWM and boost control curves showing maximum constant boost envelopes.

In reality, the maximum boost control follows the upper and lower envelope formed by the three modulation curves shown in Fig. 9. Unfortunately, the figure shows that V_{ref} on opposite sides of the zero voltage line are generally different causing the boost to vary with every cycle of the carrier wave, which is unacceptable for control. Boost is roughly proportional to $T_o/T_{carrier}$. From [8], considering the range $30^\circ \leq \theta \leq 90^\circ$, the average value for the shoot-through duty cycle is

$$\frac{T_o}{T_{carrier}} = 1 - M_{shoot-through} = 1 - \frac{(M \sin \theta - M \sin(\theta - 2\pi / 3))}{2} = 1 - \frac{\sqrt{3}}{2} M \cos(\theta - \pi / 3) . \quad (16)$$

The minimum value of $T_o/T_{carrier}$ occurs for $\theta = 60^\circ$, where V_{ref} is the average of equal positive and negative modulation voltages. The maximum value occurs for $\theta = 30^\circ$ and 90° , where V_{ref} is the average of unequal positive and negative modulation voltages, which means that one of its shoot-through duty cycles will infringe on PWM operation. From (16) and knowing that the minimum value of $T_o/T_{carrier}$ is $1 - M\sqrt{3}/2$ and that it does not infringe on PWM operation, one may construct upper and lower constant boost control reference curves whose difference is $M\sqrt{3}$, which leads to an average constant value of $V_{ref} = M\sqrt{3}/2$. This in turn leads to the desired maximum constant shoot-through duty cycle,

$$\frac{T_o}{T_{carrier}} = 1 - \frac{\sqrt{3}}{2} M \quad . \quad (17)$$

From (16) the expressions for boost, B , and gain, G , follow as

$$B = \frac{1}{\sqrt{3M - 1}} \quad (18)$$

and

$$G = \frac{M}{\sqrt{3M - 1}} \quad . \quad (19)$$

These expressions, which are plotted in Fig. 10, show that a high gain requires small values of M and that, unfortunately, small values of M lead to large boost which places greater voltage stress on the inverter switches.

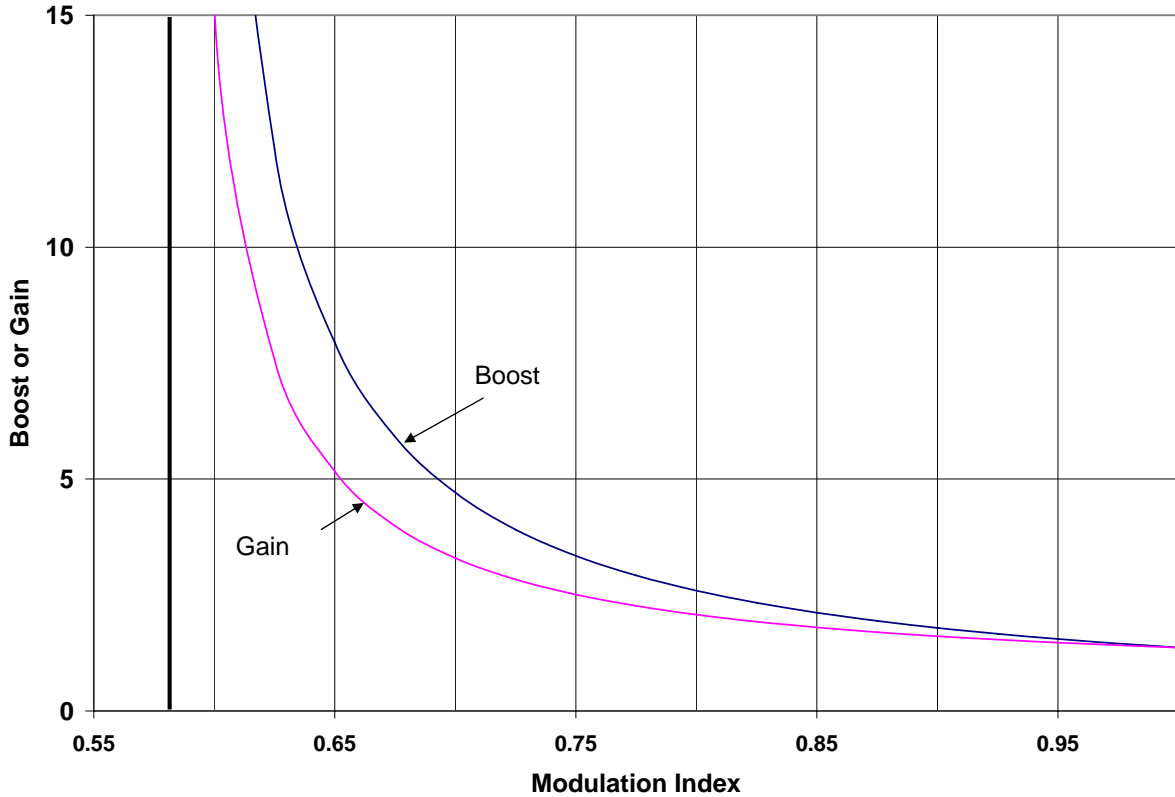


Fig. 10. Relation of boost and gain to PWM index.

The total switching device power (SDP) of a traditional PWM inverter, a dc-dc boosted PWM inverter, and a Z-source inverter were calculated and compared showing that the Z-source reduces the total average SDP by 15%, which means lower cost [10]. In the same paper, the

motor voltage produced by Z-source inverters, when subjected to the same switch voltage stress as traditional PWM inverters, was 1.55 times greater than that produced by a conventional PWM inverter. Simulation models of the three types of inverters were used to confirm the validities of the efficiency comparisons, which showed that the Z-source inverter can increase inverter conversion efficiency by 1% over the traditional and dc-dc boosted PWM inverters.

The analysis in [4] and [10] considered that during shoot-through the current, which is twice the current through the inductor, passes in parallel through all three legs of the inverter. A paper analyzing PWM operation of a Z-source inverter [11] concluded that under space vector control, for which only one switch could be changed per state, the entire shoot-through current would flow through only one phase, which increases the current stress on the switches as well as the SDP.

DISCUSSION

Figure 11 is a schematic similar to the first Toyota Hybrid System (THS) used in the Prius. It employed a large propulsion battery pack whose voltage was close to 300V and its power rating was 33 kW. The lines with arrows indicate the power flow. A dc-dc converter is included in this schematic to maintain the SOC on the battery that powers all of the accessory systems. The THS and THSII employ a 12-V auxiliary voltage system; however, the HEV developers are also considering a 42-V system.

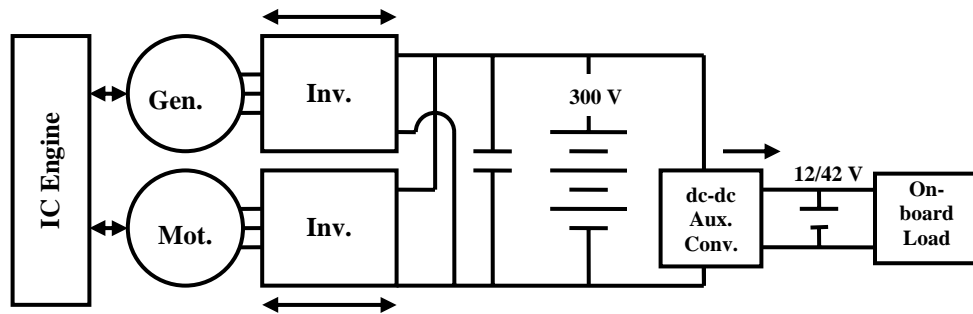


Fig. 11. Schematic similar to THS.

Toyota made a significant advance with their THSII system and Fig. 12 is a schematic similar to the THSII system. It employed a smaller 200-V propulsion battery and added a boost converter to match the propulsion battery's voltage to an increased motor voltage of 500 V, which delivered more power without increasing the current resulting in higher efficiency. Using a boost converter to match the battery voltage with the inverter link voltage, 20 kW of power from the smaller propulsion battery could be added to 30 kW from the generator to supply the larger rated power of 50 kW, which is 50% higher than that of the THS. The THSII also optimizes its output voltage according to the relative state of the motor and generator, which helps decrease both switching losses in the inverter and copper losses in the inductor and boost converter by decreasing the ripple current. The efficiency of the motor and inverter are optimized by setting the variable system voltage such that flux-weakening control is not required and system losses are minimized. These modifications, as well as increasing the operating speed of the generator

from 6500 to 10,000 rpm, have enabled Toyota to maintain the same physical size for the ac synchronous motor and generator and increase the overall efficiency.

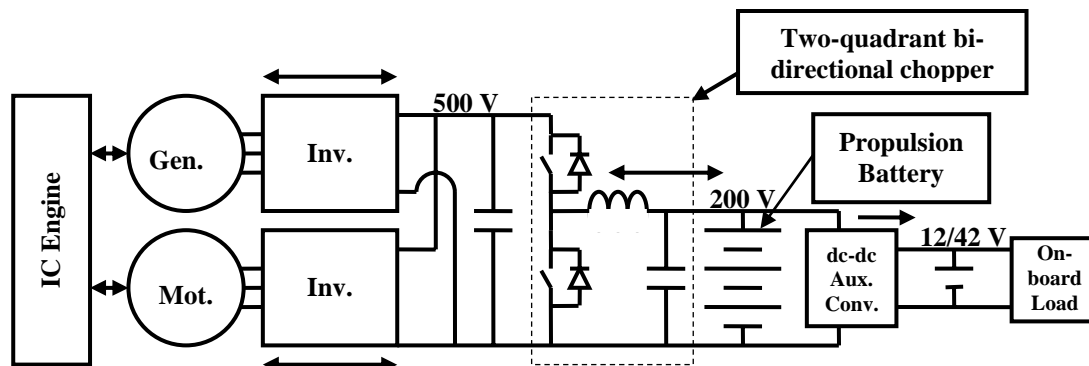
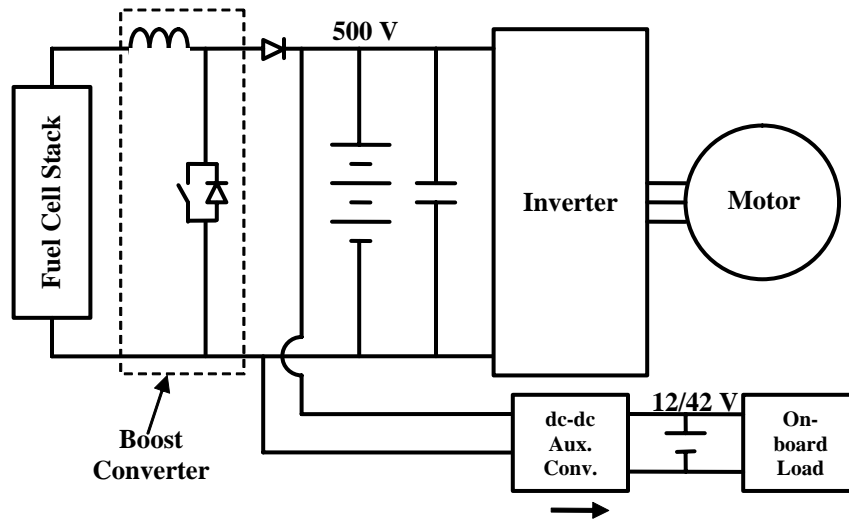


Fig. 12. Schematic similar to THSII.

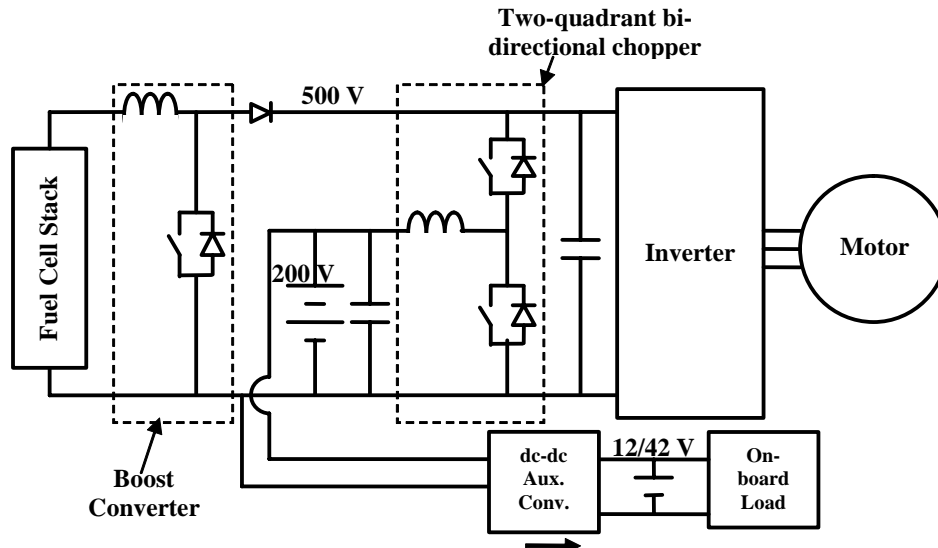
The Z-source inverter is better suited for integration into FC powered electric vehicles (EVs) because it can maintain the necessary voltage to the electric motor even when the FC voltage drops as the current load increases. For an ICE powered vehicle, the Z-source inverter can boost a lower voltage battery but it is necessary to add an extra auxiliary battery and difficult to connect all regeneration sources, such as brakes and generator, to maintain the SOC on all batteries.

Since the Z-source inverter is better suited for integration into FC powered EVs, we shall consider FC powered applications first followed by ICE powered applications. A hybrid configuration, which employs a secondary power source, will be examined as we explore integration of the Z-source inverter and examine the number of components in the various circuits. Note that each configuration has a dc-dc buck converter to maintain the SOC of an auxiliary battery necessary to meet on-board load demands. Each FC configuration must also be able to operate a compressor motor expanding unit (CMEU) from either a propulsion battery whose voltage is sufficiently high or from an auxiliary battery with a dc-dc boost converter.

Four FC applications will be examined. The first two are conventional FC configurations shown in Fig. 13. Note that some type of boost converter must be used to compensate for the FC voltage drop as the current draw increases. In Fig. 13, the first configuration has a high voltage secondary energy propulsion battery for close comparison with the Z-source FC configuration, which also has a high voltage battery. The second has a low voltage secondary energy propulsion battery similar to the THSII. The third, shown in Fig. 14, is a simple non-HEV application with a generator to maintain an auxiliary battery's SOC. The fourth is a more complex FC HEV whose configuration is being studied at Michigan State University (MSU) by Fang Peng [13]. Then we shall examine some of the difficulties of using the Z-source inverter with and ICE.

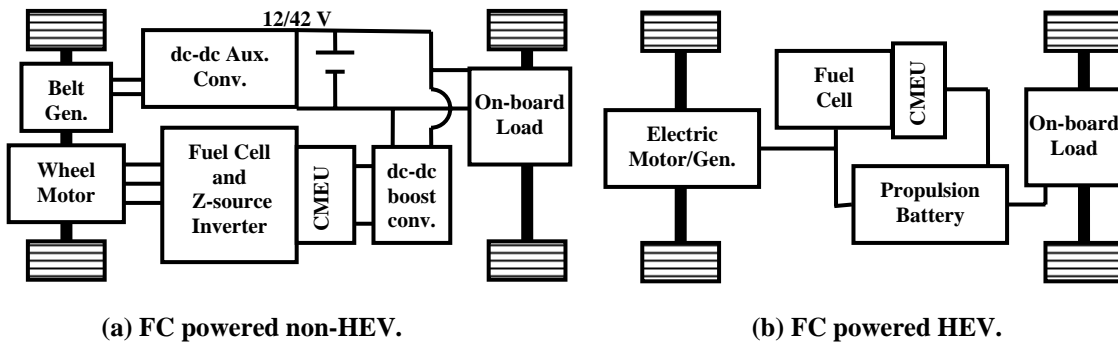


a. High voltage secondary energy propulsion battery.



b. Low voltage secondary energy propulsion battery (similar to THSII).

Fig. 13. Conventional boost converter configuration of a FC powered HEV.



(a) FC powered non-HEV.

(b) FC powered HEV.

Fig. 14. Simple and complex FC powered EVs.

Figure 14(a) shows a simple non-HEV powered by a FC with no regenerative energy capture from the wheel motor. A belt driven generator is used to maintain the SOC on a 12/42 V accessory battery as for today's automobiles. An additional dc-dc boost converter drives the compression motor expansion unit as the FC is brought on line. On the right is a noncommittal schematic of a FC powered HEV. It is hybrid like the THSII because it has a secondary power source, which is the propulsion battery. Propulsion battery power can combine with FC power to deliver rated power. It is possible that the propulsion battery voltage is sufficiently large that it can operate the air pump directly. The right schematic is conceptual not showing power flow details.

There are two possible places to insert a propulsion battery in a FC powered HEV driven by a Z-source inverter. The configuration shown in Fig. 15 is now under study [13]. In it a battery is inserted in parallel with either one of the two Z-circuit capacitors because of circuit symmetry. The capacitor must remain across the battery terminals to absorb ripple currents, which shorten the battery life. In both cases, if the average voltage is E_b , the link voltage gain is

$$\frac{v_i}{V_o} = \left(\frac{I}{T_o / T_{Carrier}} - I \right) \left(\frac{E_b}{V_o} - I \right), \quad (20)$$

where $T_o/T_{carrier}$ is the shoot-through duty cycle. Thus the battery, whose voltage must exceed V_o , must be a high voltage battery and the battery voltage must exceed the FC voltage. The inverter module may be operated in the same way as traditional inverters to maintain the battery SOC with excess power from the FC and from regenerative braking. Furthermore, the high voltage across the propulsion battery is sufficient to operate the CMEU thereby eliminating the dc-dc boost converter.

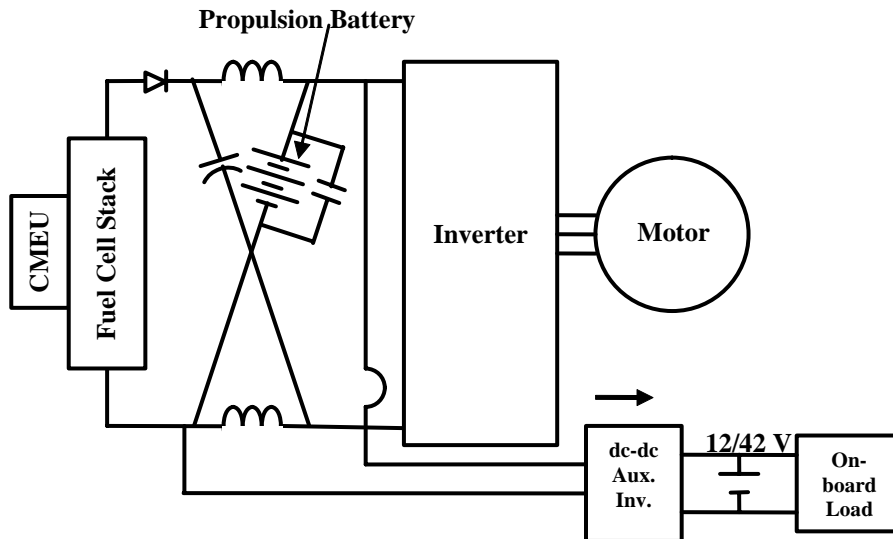


Fig. 15. Proposed configuration of a Z-source inverter driven FC HEV.

Although the Z-source inverter was developed in the search for a better FC drive system, it poses a question about applying its boost feature in a traditional ICE powered HEV. Figure 16 shows

one such configuration. The propulsion battery is connected so that it can be used to drive the starter/generator as a starting motor for the ICE. The Z-source inverter boosts the voltage from a 200-V storage battery to 500 V for improved motor efficiency. The ICE can deliver power directly to the traction wheels and to the generator as in today's HEVs. The figure, however, illustrates some of the difficulties in applying the Z-source inverter to an ICE powered HEV. Although the 200-V propulsion battery provides a secondary source of power, it cannot receive regenerated braking power from the motor because of the intervening blocking diode required to isolate the 500 V link from the 200 V battery. In this configuration, the only available regenerated power to maintain the battery SOC must pass through the starter motor/generator. Further, since the generator is connected to maintain the SOC on the secondary energy propulsion battery, it incurs additional losses because current must pass through the Z-sources' diodes when it is being used to provide drive power. If the generator were connected directly to the high voltage link, there would be no way to maintain the SOC on the propulsion battery. This might be accommodated by switching the generator connection between the low voltage and high voltage buses depending upon whether it is charging or driving; however, this adds a complication.

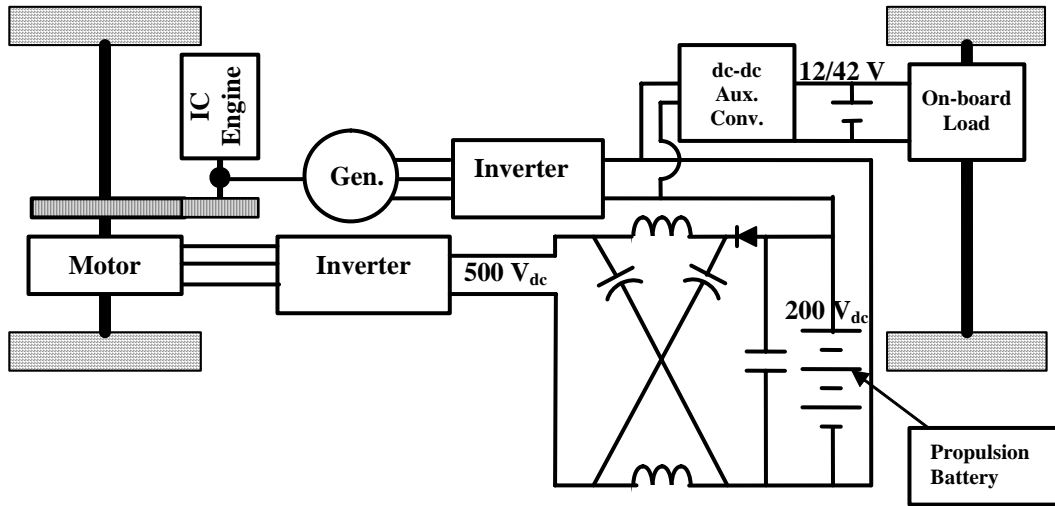


Fig. 16. A configuration of an ICE powered HEV driven by a Z-source inverter.

Table 1 summarizes the number of components in each configuration. The figure showing the schematic is identified in the first column. Each inverter contains six semiconductor switches. Each semiconductor switch has an anti-parallel diode. The components in the dc-dc auxiliary converter, which charges the battery that supplies the on-board load, are common to all of the configurations and are not counted in the table. However, when the dc-dc auxiliary converter is supplied by a lower V-source, such as a 200V propulsion battery, its components can have a lower rating than when it is supplied by a 500V link, which reduces component costs. The CMEU, which must operate when the FC stack is started, may receive its power from a dc-dc boost converter that raises the voltage of a 12/42-V accessory battery to 200 V. Alternately, if it can be driven directly by a 200V propulsion battery, the cost of a dc-dc boost converter can be eliminated.

Table 1. Component count for several HEV configurations with and without voltage boost

HEV and converter type	Switches	Inductors	Caps	Propulsion battery	dc-dc converter for CMEU^(a)
EV – battery powered	6	0	1	1	NA^(b)
HEV – ICE powered with secondary energy source					NA
Prius THS (Fig. 11)	12	0	1	1	NA
Prius THS II (Fig. 12)	14	1	2	1	NA
Proposed HEV with Z-source Converter (Fig. 16)	12	1^(c)	3	1	NA
EV – FC powered (Fig.14.a)	6	1^(c)	2	0	YES
HEVs – FC powered with secondary energy source					
Traditional boost converter with high voltage propulsion battery (Fig. 13.a.)	7	1	1	1	NO
Traditional boost converter with low voltage propulsion battery (Fig. 13.b)	9	2	2	1	NO
Proposed Z-source with a high voltage battery in parallel with one capacitor (Fig. 15)	6	1^(c)	2	1	NO

(a) CMEU is the compression motor expansion unit which must operate during startup of the FC.

(b) NA means not applicable.

(c) The inductor in the Z-source inverter is physically one, although functionally two because it has two windings on a shared core.

The proposed HEV configuration, powered by an ICE with a Z-source inverter (Fig. 16) instead of a two-quadrant bi-directional chopper feeding a PWM inverter, reduces the number of switches by two and maintains one inductor by sharing a common core. The switch saving is notable, but the blocking diode necessary to keep the 500-V link from discharging back into the 200-V propulsion battery introduces operational losses.

If one decides that a secondary power source is not necessary, the simple FC driven EV with no regenerative braking from the wheels becomes attractive. A belt or direct driven generator is used to maintain the SOC of a 12/42-V accessory battery whose voltage provides for the on-board loads and is boosted by a dc-dc converter to drive the CMEU during startup. The saving is elimination of the propulsion battery, but this configuration has no secondary backup power.

The following discussion provides rough estimates of cost benefits under an umbrella of certain assumptions. More reliable estimates require more details about the actual components that will be used in the circuitry, which are suggested by researchers for original equipment manufacturers (OEMs) to review and choose as they decide which products they will market. The most reliable estimates depend upon the quantity purchased, and that level of detail, which must be provided by the vendor, is understandably reserved for the best potential OEM customers.

Nevertheless, the cost benefit of configurations in Table 1 may be estimated under the umbrella of information provided by some vendors, who have been subcontracted by DOE, and by university researchers, who are developing inverters. An example of such information is the percentage cost of semiconductor devices, capacitors, and inductors. Three vendors estimated that the semiconductor devices cost 25%, 30%, and 21% of the total inverter cost respectively, which averages as 25.3%. The same three vendors estimated that the capacitor costs would be 11.5%, 9.9%, and 18% respectively, which averages as 13%. This indicates a greater potential for savings associated with semiconductor devices. A comparison of traditional inverters and Z-source inverters for FCs [10] and the \$185 inductor cost [15] obtained from Miaosen Shen and Fang Peng at MSU reduced by 60% to \$74 anticipated from quantity production provided a cost ratio of the power build modules for a traditional PWM inverter, a PWM inverter fed by a traditional boost converter, and a Z-source inverter. The traditional PWM inverter's semiconductor power module cost of \$808 was for three dual packs rated at 600V/400A. The traditional boost converter's semiconductor cost of \$270 was for one dual pack rated at 600V/400V feeding a traditional PWM inverter whose semiconductor cost was \$240 for a six pack rated at 600V/200A. Addition of an inductor yielded a total cost of \$584. The Z-source inverter's semiconductor power module cost of \$309 was for a six pack rated at 600V/300A. Addition of an inductor yielded a total cost of \$383. This ratio is 1 : 0.710 : 0.474 .

One may assume that each capacitor added to the EV configuration will add roughly an equal amount to the cost. Even though additional small capacitors are across batteries to reduce high frequency ripple they are usually film capacitors, which are about 1.6 times more expensive than electrolytic capacitors based on off-the-shelf prices. Doubling and tripling the number of capacitors will raise their cost percentage from 13% to 23% and 31% of the inverter cost respectively. For an inverter cost of \$1340 the corresponding capacitor cost increases are \$174 and \$348.

One may compare the costs of the power build sections of each configuration. The power build section contains the semiconductors in the inverters that drive the motor and the generator, the semiconductors in the boost converter or in the chopper, and the inductances needed by the chopper, traditional boost converter, and Z-source inverter. These numbers are based on vendor quotes for 1000–1999 units for three levels of semiconductor packs [16]. Current in conventional PWM motor inverters and in traditional boost converters that feed PWM inverters require 600V/400A dual packs at \$269.60 each. Current in the starter/generator inverter drives and in the PWM inverter fed by a traditional boost converter only require 600V/200A six packs at \$240 each. Current in the Z-source inverters employed 600V/300A six packs at \$308.88 each.

Now we shall look at some cost comparisons for different power build sections. There is a general consensus among those who have studied the THSII that it is the current baseline with

the most desirable features. Its power build section estimated cost is \$1392. The power build sections estimated cost difference between THSI and THSII is \$343, which is an estimate of what Toyota was willing to pay to obtain and improve reliability and to deliver 50% more power without changing the motor/drive size. What stands out in Table 2 is the drop in cost of the power build section when FCs replace the ICE as the primary energy source. The power build section of the FC powered HEV with a traditional boost converter and a bi-directional chopper comparable THSII costs about \$996, which is \$396 less than the THSII.

Most notable, however, is the dramatic reduction of the power build section cost to \$383 for the FC powered Z-source inverter with a high voltage battery as a secondary energy source in parallel with one of the two capacitors. This power build section cost is \$666 below the THSI cost and \$1009 below the THSII cost. Furthermore, it is \$201 less than the power build section cost of the conventional FC inverter, which is fed by a traditional boost converter.

Table 2. Estimated cost of power build section of several EV and HEV inverter configurations

Type	Fig.	Feature	Primary/ secondary energy	Type boost	Power Build Section						Total cost	Related component
					No. of inductors	Switches	Switch package	No. units	Cost each, \$			
EV	–	Basic	Battery/ None	None	0	6	dual	3	269.60	\$809	Motor	
HEV	11	THSI	ICE/ Battery	None	0	12	Dual Six	3 1	269.60 240.00	\$1049	Motor Generator	
	12	THSII	ICE/Battery	Chopper	1	14	Dual Dual Six	3 1 1 1	269.60 269.60 240.00 74.00	\$1392	Motor Chopper Generator Inductor	
	16	Not well behaved in regen.	ICE/Battery	Z-source	1	12	Dual Six	3 1 1	269.60 240 74.00	\$1123	Motor Generator Inductor	
EV	14(a)	No regen. Hypothetical	FC/ none	Z-source	1	6	Six	1 1	308.88 74.00	\$383	Motor Inductor	
HEV	13(a)	Traditional boost	FC/ High voltage battery	Traditional boost	1	7	Six Dual	1 1 1	240.00 269.60 74.00	\$584	Motor Boost conv. Inductor	
	13(b)	Bi- directional chopper	FC/ Medium voltage battery	Traditional Boost and Bi-direct. chopper	2	9	Six Dual Dual	1 1 1 2	308.88 269.60 269.60 74.00	\$996	Motor Boost Chopper Inductor	
	15	Z-source - under study at MSU	FC/ High voltage battery	Z-source	1	6	Six	1 1	308.88 74.00	\$383	Motor Inductor	

CONCLUSIONS

Use of a two-quadrant bi-directional chopper by Toyota allowed them to: (1) increase the dc link voltage to 500 V which improved the motor efficiency; (2) supply power to that link from a smaller battery pack, whose voltage was reduced from 270 V to 200V; and (3) increase the power output by 50% without changing the motor dimensions. Components added to the THS system by the THSII chopper are an inductor, two switches, and a capacitor.

The recent invention of the Z-source inverter provides a new technology that can eliminate the switch in the traditional boost converter between the FC and the high voltage dc link (Fig. 13(a)). It can also eliminate the two additional switches between a moderate 200-V secondary energy storage voltage and a high 500-V traction motor voltage (Fig. 13(b)) similar to that used in the THSII system. It eliminates all danger from shoot-through, which short circuits the supply voltage through the inverter switches, destroying switches in a traditional inverter. Instead, it makes double use of the zero-state time to boost the voltage as well as control the average voltage. Components introduced by the FC powered Z-source inverter with a battery replacing one of the capacitors over the traditional boost converter are two small inductors to replace one large inductor with little cost difference. Component savings are one less capacitor and one less switch.

Brake regeneration is normally considered important for HEVs; however, if one decides that neither brake regeneration nor a secondary power source is necessary, a non-hybrid FC powered EV with direct electrical connection to a high voltage electric motor by a Z-source inverter becomes attractive. In this configuration, a belt driven generator could maintain the SOC of the accessory energy storage just like a conventional automobile. A dc-dc boost converter could raise the accessory voltage to the 300 V level to drive the CMEU. This unadorned system has only six switches, two small inductors, and no propulsion battery. It will get you there but can't limp home if repair is necessary.

The ICE or the FC must supply power to more than the traction motor. Hybrid ICE and FC HEVs must supply power to charge a 12/42-V auxiliary storage battery and a 200 V or 500 V secondary energy storage system. The energy storage system supplements the power from the ICE or FC allowing the vehicle to deliver rated power during high load conditions. If the Z-source inverter is applied to both the hybrid ICE and FC HEVs, the challenge is to connect it to the power source without interfering with its shoot-through boost operation.

A Z-source inverter, which has the least number of components, will directly drive a non-hybrid FC vehicle (Fig. 14(a)) provided regenerative braking and secondary energy storage are not needed. The SOC of the auxiliary battery would be maintained with a small alternator like those used in today's automobiles. This configuration would require a dc-dc converter to operate the CMEU from the auxiliary battery.

Either capacitor in the Z-source inverter may be paralleled with a battery to provide the secondary energy source in a FC vehicle. A high voltage battery is necessary; however, it may be small if fewer ampere-hours are required. Brake regenerative power and excess FC power may be used to maintain the high voltage battery's SOC and the CMEU can be operated directly

from the high voltage battery. The dc-dc converter to the auxiliary battery must draw its power from the high voltage link.

Attempts to apply the Z-source inverter to an ICE powered HEV (Fig. 16) revealed that Z-source technology doesn't migrate naturally into conventional ICE powered HEV configurations. First, the FC is replaced by a low voltage propulsion battery, which doesn't have the dramatic voltage drop exhibited by the FC as the load increases. Although the 200-V low voltage propulsion battery in Fig. 16 can provide a secondary source of power, it cannot receive regenerated braking power from the motor because of the intervening blocking diode required to isolate the 500-V link from the 200-V battery. In this configuration, the only available regenerated power to maintain the battery SOC must pass through the generator. Further, since the generator is connected to maintain the SOC on the secondary energy propulsion battery, it incurs additional losses when in drive mode because current must pass through the Z-source inverter's blocking diode. If the generator were connected directly to the high voltage link, there would be no way to maintain the SOC on the propulsion battery, again because of the intervening diode. This might be accommodated by switching the generator connection between the low voltage and high voltage buses depending upon whether it is charging or driving; however, this adds a significant control complication and more hardware. For today's commercial HEV technology the simple two-quadrant, bi-directional chopper shown in Fig. 12 provides a cheap effective and efficient way to drive and maintain battery SOC without complex additional circuits.

Further, as we explored the potential to replace the two-quadrant bi-directional chopper by the boost technology of a Z-source inverter, we found a straightforward modular replacement is complicated by the Z-circuit's integration requirements. The problem is that the connecting lines must be very short so that they do not introduce unacceptable inductance because the inductance cannot be easily compensated by snubber caps without affecting shoot-through operation of the Z-source. Consequently we conclude that, based on today's understanding, the Z-source inverter is not well suited for use in ICE powered HEVs.

A cost estimate of ICE and FC power build sections, which includes semiconductor and inductor costs, indicates the cost penalty accepted by Toyota to achieve the benefits of the THSII over THSI and shows the potential for a FC powered HEV with a Z-source inverter to reduce inverter cost. The THSII, which is the current baseline with the most desirable features, has an estimated power build section cost of \$1392. The power build sections estimated cost difference between THSI and THSII is \$343, which is an estimate of what Toyota was willing to pay to obtain and improve reliability and to deliver 50% more power without changing the motor/drive size. There is a large drop in cost of the power build section when FCs replace the ICE as the primary energy source. The power build section of the FC powered HEV with a traditional boost converter and a bi-directional chopper comparable THSII costs about \$996, which is \$396 less than the THSII. Most notable, however, is the dramatic reduction of the power build section cost to \$383 for the FC powered Z-source inverter with a high voltage battery as a secondary energy source in parallel with one of the two capacitors. This power build section cost is \$666 below the THSI cost and \$1009 below the THSII cost. Furthermore it is \$201 less than the power build section cost of the conventional FC inverter, which is fed by a traditional boost converter.

REFERENCES

1. N. Mohan, T. Undeland, and W. Robbins, *Power Electronics: Converters, Applications, and Design*, Chapter 5, John Wiley and Sons, Inc., 1989.
2. F. Z. Peng, "Z-source Inverter," *IEEE Transactions of Industry Applications*, **39**(2), March/April 2003.
3. F. Z. Peng, et al., "Z-source Inverter for Adjustable Speed Drives," pp. 33–35 in *IEEE Power Electronics Letters*, **1**(2), June 2003.
4. J. W. McKeever, S. Das, L. M. Tolbert, and L. D. Marlino, "Life-Cycle Cost Sensitivity to Battery-Pack Voltage of an HEV," Paper 00FCC-17, 2000 Future Car Congress, Arlington, Virginia, April 4, 2000.
5. M. Okamura, E. Sato, and S. Sasaki, "Development of Hybrid Electric Drive System Using a Boost Converter," EVS-20, Session 5, The 20th International Electric Vehicle Symposium and Exposition, Long Beach, California, November 15–19, 2003.
6. B. Ozpineci, et al., "Optimum Fuel Cell Utilization with Multilevel DC-DC Converters," pp. 1572–1576 in *Conference Proceedings of the 19th Annual IEEE Applied Power Electronics Conference and Exposition*, **3**, 2004.
7. F. Z. Peng, "Z-source Inverter for Motor Drives," pp. 249–254 in *The 35th Annual IEEE Power Electronics Specialists Conference*, **1**, Aachen, Germany, June 20–25, 2004.
8. F. Z. Pang, et al., "Maximum Boost Control of the Z-Source Inverter," pp. 255–260 in *The 35th Annual IEEE Power Electronics Specialists Conference*, **1**, Aachen, Germany, June 20–25, 2004.
9. M. Shen, et al., "Maximum Constant Boost Control of the Z-source Inverter," pp. 142–147 in *Proceedings of the 39th Annual IEEE Industrial Applications Society*, **1**, October 3–7, 2004.
10. M. Shen, et al., "Comparison of Traditional Inverters and Z-Source Inverter for Fuel Cell Vehicles," pp. 125–132 in *Proceedings of Power Electronics in Transportation*, October 21–22, 2004.
11. P. Chaing Loh, et al., "Pulse-Width Modulation of Z-Source Inverters," pp. 148–155 in *Conference Record of the 39th Annual IAS Meeting*, **1**, October 3–7, 2004.
12. K. Yoon-Ho, et al., "Z Fuel Cell System with Z-Source Inverters and Untracapacitors," pp. 1587–1591 in the *Record of the 4th International Conference on Power Electronics and Motion Control*, **3**, August 14–16, 2004.
13. F. Z. Peng, personal email communication.
14. G. J. Su, et al., "A Low Cost, Triple Voltage Bus DC/DC Converter for Automotive Applications," 20th Annual Power Electronics Conference and Exposition, 2005.
15. Miaosen Chen, personal email communication.
16. Fang Z. Peng, "Z-Source Inverter for Hybrid Electric and Fuel Cell Powered Vehicles," slide 13 of presentation at DOE FreedomCAR and Vehicle Technologies Program Annual Review of Advanced Power Electronics and Electrical Machines, June 7–9, 2004.

DISTRIBUTION

Internal

1. D. J. Adams
2. C. W. Ayers
3. T. A. Burress
4. S. L. Campbell
5. C. L. Coomer
6. E. C. Fox
7. K. P. Gambrell
8. J. S. Hsu
9. P. A. Jallouk
10. K. T. Lowe
11. S. C. Nelson
12. L. D. Marlino
13. M. Olszewski
14. R. H. Wiles
- 15–16. Laboratory Records

External

17. T. Q. Duong, U.S. Department of Energy, EE-2G/Forrestal Building, 1000 Independence Avenue, S.W., Washington, D.C. 20585.
18. R. R. Fessler, BIZTEK Consulting, Inc., 820 Roslyn Place, Evanston, Illinois 60201-1724.
19. K. Fiegenschuh, Ford Motor Company, Scientific Research Laboratory, 2101 Village Road, MD-2247, Dearborn, Michigan 48121.
20. V. Garg, Ford Motor Company, 15050 Commerce Drive, North, Dearborn, Michigan 48120-1261.
21. E. Jih, Ford Motor Company, Scientific Research Laboratory, 2101 Village Road, MD-1170, Rm. 2331, Dearborn, Michigan 48121.
22. W. C. Johnson, University of Tennessee-Knoxville, ECE Department, 414 Ferris Hall, 1508 Middle Drive, Knoxville, Tennessee 37996.
23. A. Lee, Daimler Chrysler, CIMS 484-08-06, 800 Chrysler Drive, Auburn Hills, Michigan 48326-2757.
24. F. Liang, Ford Motor Company, Scientific Research Laboratory, 2101 Village Road, MD1170, Rm. 2331/SRL, Dearborn, Michigan 48121.
25. M. W. Lloyd, Energetics, Inc., 7164 Columbia Gateway Drive, Columbia, Maryland 21046.
26. Brenda Medellon, USCAR, brenda@uscar.org
27. M. Mehall, Ford Motor Company, Scientific Research Laboratory, 2101 Village Road, MD-2247, Rm. 3317, Dearborn, Michigan 48124-2053.
28. J. Rogers, Chemical and Environmental Sciences Laboratory, GM R&D Center, 30500 Mound Road, Warren, Michigan 48090-9055.
29. S. A. Rogers, U.S. Department of Energy, EE-2G/Forrestal Building, 1000 Independence Avenue, S.W., Washington, D.C. 20585.
30. G. S. Smith, General Motors Advanced Technology Center, 3050 Lomita Boulevard, Torrance, California 90505.
31. E. J. Wall, U.S. Department of Energy, EE-2G/Forrestal Building, 1000 Independence Avenue, S.W., Washington, D.C. 20585.
32. B. Welchko, General Motors Advanced Technology Center, 3050 Lomita Boulevard, Torrance, California 90505.
33. P. G. Yoshida, U.S. Department of Energy, EE-2G/Forrestal Building, 1000 Independence Avenue, S.W., Washington, D.C. 20585.